# Influence of visco-Pasternak foundation parameters on the bending and vibrational behavior of thick isotropic plates

*Hebali* Habib[a], *Djidar* Fatima Zohra[b], *Derras* Abdelhak[c]

[a] Mustapha Stambouli University, Department of Civil Engineering, Mascara, People's Democratic Republic of Algeria
e-mail: habib.hebali@univ-mascara.dz,
ORCID iD: https://orcid.org/0009-0001-1309-2595

[b] Mustapha Stambouli University, Department of Civil Engineering, Mascara, People's Democratic Republic of Algeria +
Smart Structures Laboratory (SSL), University of Ain Temouchent, Ain Temouchent, People's Democratic Republic of Algeria
e-mail: fatima.djidar@univ-mascara.dz, **corresponding author**,
ORCID iD: https://orcid.org/0009-0006-6361-073X

[c] Ahmed Ben Bella University – Oran 1, Department of Chemistry, Oran, People's Democratic Republic of Algeria +
Smart Structures Laboratory (SSL), University of Ain Temouchent, Ain Temouchent, People's Democratic Republic of Algeria
e-mail: abdelhakderrasderras@gmail.com,
ORCID iD: https://orcid.org/0009-0006-2459-6461

https://doi.org/10.5937/vojtehg74-59632

FIELD: civil engineering
ARTICLE TYPE: original scientific paper

*Abstract:*

*Introduction/purpose: This study primarily aims to investigate the effect of viscoelastic Pasternak foundation parameters on the bending and free vibrational behavior of simply supported thick isotropic plates using a two-variable high-order shear deformation theory (HSDT). The theory adopted in this study uses a limited number of unknowns and avoids the use of shear correction factors to ensure zero transverse shear stresses at the surface of the plates, which is not the case with other higher-order theories that generally involve four or five unknowns. In addition, the stress and displacement responses are analyzed under uniformly distributed loads (UDLs) and sinusoidally distributed loads (SDLs). Moreover, natural frequencies corresponding to both bending and thickness-shear modes are provided to demonstrate the accuracy of the proposed model in predicting the dynamic behavior of simply supported isotropic square and rectangular plates.*

*Methods: The main contribution of this work lies in the integration of the effects of elastic foundation parameters and damping coefficients on the bending and vibration responses of simply supported thick isotropic plates, using a refined two-variable high-order shear deformation theory. In*

*addition, the formulation of the displacement field introduces a number of undetermined integral terms, hence reducing the number of unknowns. The governing equations are derived using Hamilton's principle. Moreover, Navier's method is utilized to determine the analytical solutions for simply supported plates, while natural frequencies are calculated by solving the corresponding eigenvalue problem.*

*Results: The analytical results are validated against several established higher-order shear deformation theories (ESDT, HSDT, TSDT), the first-order shear deformation theory (FSDT), and the classical plate theory (CPT). The findings show excellent agreement when viscoelastic and foundation effects are not taken into account. It is important to emphasize that when these effects are considered, the results show increased plate stiffness, leading to lower deflections and higher natural frequencies.*

*Conclusion: The proposed theory provides results in close agreement with those obtained from existing models. It also clearly highlights the significant influence of viscoelastic foundation parameters on both the static and dynamic behavior of isotropic plates.*

*Key words: bending, vibration, isotropic plate, visco-Pasternak foundations.*

## Introduction

Nowadays, plates are widely used in industry and several emerging technological fields, such as aeronautics, marine engineering, civil engineering, and mechanical engineering. It has been revealed that transverse shear and normal deformation effects are quite significant in shear-flexible plates. These plates can be made of isotropic, orthotropic, anisotropic, or laminated composite materials.

Furthermore, the behavior of plates subjected to mechanical and thermal loads can generally be predicted using either a three-dimensional (3D) elasticity theory or other equivalent single-layer (ESL) elasticity theories. These ESL theories can take into account the transverse shear and normal deformation effects, depending on the assumptions considered. It should be noted that the classical plate theory (CPT) is the simplest ESL model. It can solely be applied to thin plates for which the shear deformation and transverse normal effects are negligible.

The first-order shear deformation theory (FSDT), which is commonly referred to as the Reissner-Mindlin theory, is the next level in the hierarchy of ESL models. This FSDT theory takes into account the shear deformation effects by assuming a linear variation of displacements through the thickness of the plate, which requires the use of a shear correction factor. According to the findings of Lanhe (2004), Chen (2005),

Park and Kim (2006), Bouazza et al. (2010), Kiani and Eslami (2012), and Yaghoobi & Yaghoobi (2013), this theory is widely used to analyze the behavior of functionally graded material (FGM) plates.

The limitations of CPT and FSDT theories have led to the development of higher-order shear deformation theories (HSDT) which eliminate the need for shear correction factors and provide a more realistic representation of shear deformation and stress variation through the plate thickness. In this regard, various applications of this theory to thick isotropic plates have been explored by Levy (1877), Stein (1986, 1989), Lee et al. (1989), Stein et al. (1990), Shimpi (2002), Ghugal and Pawar (2011), Ghugal and Sayyad (2011), Sayyad and Ghugal (2012), and Djidar et al. (2022).

Likewise, Soldatos (1992), Chen et al. (2009), Xiang et al. (2011), Mantari et al. (2012), Mantari and Guedes Soares (2012), Xiang and Kang (2013), Wattanasakulpong et al. (2013), Grover et al. (2013), and Mantari et al. (2014) carried out a large number of studies to investigate composite and functional gradient (FG) plates using higher-order shear deformation theories (HSDT).

It is worth noting that plates resting on elastic foundations are commonly encountered in various civil and structural engineering sectors. It has been established that the simplest and most commonly used model for characterizing the interaction between the plate and supporting medium is that of Winkler, as this model represents the foundation as an array of independent vertical springs without any shear interaction (Winkler, 1867).

On the other hand, to make this approach more realistic, Pasternak (1954) introduced a two-parameter foundation model by adding a shear layer to the stiffness of the vertical spring, which allows for interaction between adjacent springs.

Likewise, several research studies have been conducted by Huang et al. (2008), Amini et al. (2009), Ait Atmane et al. (2010), Ameur et al. (2011), Baferani et al. (2011), Fallah et al. (2013), Sobhy (2013), Hebali et al. (2014), Mahi et al. (2015), Saidi et al. (2016), and Benahmed et al. (2017) to examine the mechanical behavior of functionally graded (FG) plates resting on a Winkler-Pasternak foundation.

More recently, attention has turned towards viscoelastic foundations, which extend the Pasternak foundation model by introducing time-dependent behavior. In addition, numerous studies have explored the mechanical response of FG beams and plates resting on viscoelastic foundations under various loading and boundary conditions.

Zeighampour and Beni (2015), they analyzed the vibrational behavior of axially functionally graded (AFG) nanobeams resting on a viscoelastic Pasternak foundation. Arani and Kiani (2018), they conducted a nonlinear free and forced vibration analysis of microbeams resting on a nonlinear orthotropic visco-Pasternak foundation, while considering various boundary conditions. Similarly, Arshid et al. (2019) employed the classical and some higher-order plate theories, such as CPT, FSDT, and TSDT, to investigate the effect of porosity on the free vibration of SPFG circular plates resting on viscoelastic Pasternak foundations. Boulefrakh et al. (2019), they mainly focused on the bending and vibration behaviors of thick FG plates, while highlighting the effect of viscoelastic foundation parameters. In this context, Bounouara et al. (2023) conducted two distinct studies. In the first one, the authors analyzed the impact of viscoelastic Pasternak foundations on the free vibration behavior of exponentially graded sandwich plates under various boundary conditions, while in the second, they primarily focused on the thermo-mechanical bending responses of anisotropic thick laminated composite plates resting on a viscoelastic foundation.

Furthermore, Bennedjadi et al. (2023) employed a refined shear deformation theory to investigate the buckling response of exponentially graded sandwich plates supported by viscoelastic foundations. Likewise, I.M. Mudhaffar (2023) proposed a quasi-3D shear deformation theory with four variables to study the bending behavior of FG plates subjected to hygro-thermo-mechanical loading and supported by viscoelastic foundations. Similarly, Frahlia (2023) used the four-unknown high-order shear deformation theory to assess the effects of viscoelastic foundation parameters on the dynamic response of FG plates.

The present study essentially aims to analyze the bending and free vibration behavior of simply supported thick isotropic plates resting on a viscoelastic Pasternak foundation. To achieve this, it was deemed appropriate to adopt a simplified higher-order shear deformation theory with only two unknowns. The viscoelastic foundation model incorporates the damping effects into the classical Pasternak foundation that is characterized by the Winkler-Pasternak shear modulus. Then, a validation study was carried out in order to assess the accuracy and reliability of the proposed theory. The results obtained showed excellent agreement with those reported in the literature.

It is worth emphasizing that, though Djidar et al. (2022) utilized the same higher-order shear deformation theory, their study did not consider plates resting on a viscoelastic foundation. The present work seeks to extend the theory to include this effect, while incorporating the Winkler

modulus (Kw), the Pasternak shear modulus (Ks), and the viscoelastic damping coefficient (Ct). In addition, a comprehensive parametric study is conducted to investigate the impact of these three viscoelastic parameters on plate deflection and natural frequencies, thereby highlighting the novelty and significance of the present research.

## Theoretical formulations

### *Plate under consideration*

An isotropic plate of length a, width b, and thickness h is considered in this study, as illustrated in Figure 1.

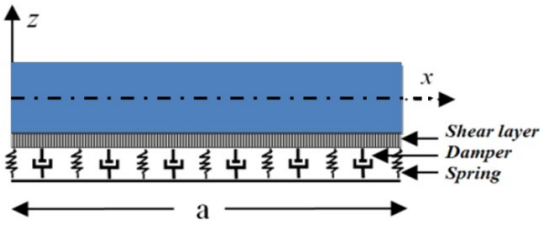



*Figure 1 – Schematic of an isotropic plate resting on visco-Pasternak foundation*

### *Kinematics and strains*

The displacement field adopted for the model under consideration is based on the formulation presented by Djidar et al. (2022). Hence,

$$\begin{aligned} u(x,y,z,t) &= -z\frac{\partial w_0}{\partial x} + K_1 f(z)\int \theta(x,y,t)\,dx \\ v(x,y,z,t) &= -z\frac{\partial w_0}{\partial y} + K_2 f(z)\int \theta(x,y,t)\,dy \\ w(x,y,z,t) &= w_0(x,y,t) \end{aligned} \tag{1}$$

where:

u, v, and w are the displacement components along the x, y, and z directions, respectively,

$w_0$ is the transverse displacement of a mid-line point of the plate, and

$\theta$ represents the rotation of the plate's cross-section due to transverse shear deformation, at the neutral axis.

In this study, the transverse shear function takes the following form, which was proposed by Karama et al. (2003):

$$f(z) = z\exp\left[-2\left(\frac{z}{h}\right)^2\right] \tag{2}$$

It is important to emphasize that the coefficients $K_1$ and $K_2$, given in (1), closely depend on the plate geometry. It is also noted that the kinematics

of Eq. (1) introduces only two unknowns ($w_0$ and $\theta$). The strain-displacement relations used in the theoretical framework adopted in this study may therefore be expressed as:

$$\begin{cases} \varepsilon_x = \dfrac{\partial u}{\partial x} = -z\dfrac{\partial^2 w_0}{\partial x^2} + k_1\theta f(z)\,, \varepsilon_y = \dfrac{\partial v}{\partial y} - z\dfrac{\partial^2 w_0}{\partial y^2} + k_2\theta f(z) \\ \gamma_{xy} = \dfrac{\partial u}{\partial y} + \dfrac{\partial v}{\partial x} = -\dfrac{\partial^2 w_0}{\partial x \partial y} + k_1\dfrac{\partial}{\partial y}\int \theta\, dx + k_2\dfrac{\partial}{\partial x}\int \theta\, dy f(z) \\ \gamma_{yz} = \dfrac{\partial v}{\partial z} + \dfrac{\partial w}{\partial y} = k_2\int \theta\, dy \dfrac{df(z)}{dz}, \gamma_{xz} = \dfrac{\partial u}{\partial z} + \dfrac{\partial w}{\partial x} = k_1\int \theta\, dx \dfrac{df(z)}{dz} \end{cases} \quad (3)$$

$$\begin{Bmatrix} \varepsilon_x \\ \varepsilon_y \\ \gamma_{xy} \end{Bmatrix} = z\begin{Bmatrix} k_x^b \\ k_y^b \\ k_{xy}^b \end{Bmatrix} + f(z)\begin{Bmatrix} k_x^s \\ k_y^s \\ k_{xy}^s \end{Bmatrix}, \begin{Bmatrix} \gamma_{yz} \\ \gamma_{xz} \end{Bmatrix} = g(z)\begin{Bmatrix} \gamma_{yz}^0 \\ \gamma_{xz}^0 \end{Bmatrix} \quad (4)$$

where:

$$\begin{Bmatrix} k_x^b \\ k_y^b \\ k_{xy}^b \end{Bmatrix} = \begin{Bmatrix} -\dfrac{\partial^2 w_0}{\partial x^2} \\ -\dfrac{\partial^2 w_0}{\partial y^2} \\ -\dfrac{\partial^2 w_0}{\partial x \partial y} \end{Bmatrix}, \begin{Bmatrix} k_x^s \\ k_y^s \\ k_{xy}^s \end{Bmatrix} = \begin{Bmatrix} k_1\theta \\ k_2\theta \\ k_1\dfrac{\partial}{\partial y}\int \theta\, dx + k_2\dfrac{\partial}{\partial x}\int \theta\, dy \end{Bmatrix} \quad (5)$$

$$\begin{Bmatrix} \gamma_{yz}^0 \\ \gamma_{xz}^0 \end{Bmatrix} = \begin{Bmatrix} k_2\int \theta\, dy \\ k_1\int \theta\, dx \end{Bmatrix}, g(z) = \frac{df(z)}{dz}$$

Navier's solution is determined in order to identify the integrals used in the proposed kinematics. This solution is thus given by the following expressions:

$$\frac{\partial}{\partial y}\int \theta\, dx = \acute{A}\frac{\partial^2\theta}{\partial x \partial y}\,, \frac{\partial}{\partial x}\int \theta\, dy = \acute{B}\frac{\partial^2\theta}{\partial x \partial y}\,, \int \theta\, dx = \acute{A}\frac{\partial\theta}{\partial x}\,, \int \theta\, dy = \acute{B}\frac{\partial\theta}{\partial y} \quad (6)$$

According to Eq. (6), in the case of the Navier approach, the coefficients $A'$ and $B'$ are taken into account depending on the type of solution used. Hence, $A'$, $B'$, $k_1$, and $k_2$ may be expressed as:

$$\acute{A} = -\frac{1}{\lambda^2}\,, \acute{B} = -\frac{1}{\mu^2}\,, k_1 = \lambda^2\,, k_2 = \mu^2 \quad (7)$$

where $\lambda$ and $\mu$ are defined in Eq.(27).

For an isotropic elastic material plate with uniform thickness, the contribution of the transverse normal stress $\sigma_z$ to the global structural response is considered negligible compared with the in-plane stresses $\sigma_x$ and $\sigma_y$. Moreover, the assumption of linear elasticity allows asserting that the in-plane stresses $\sigma_x$ and $\sigma_y$ are directly associated with the normal strains $\varepsilon_x$ and $\varepsilon_y$, while the shear stresses $\tau_{xy}$, $\tau_{yz}$ and $\tau_{xz}$ are related to the corresponding shear strains $\gamma_{xy}$, $\gamma_{yz}$ and $\gamma_{xz}$ through the constitutive relations given below.

$$\begin{aligned}\sigma_x &= \frac{E}{(1-\nu^2)}\left[\varepsilon_x + \nu\varepsilon_y\right] = \frac{E}{(1-\nu^2)}\varepsilon_x + \frac{E\nu}{(1-\nu^2)}\varepsilon_y \\ \sigma_y &= \frac{E}{(1-\nu^2)}\left[\varepsilon_y + \nu\varepsilon_x\right] = \frac{E}{(1-\nu^2)}\varepsilon_y + \frac{E\nu}{(1-\nu^2)}\varepsilon_x \\ \tau_{xy} &= \frac{E}{2(1+\nu)}\gamma_{xy}, \tau_{xz} = \frac{E}{2(1+\nu)}\gamma_{xz}, \tau_{yz} = \frac{E}{2(1+\nu)}\gamma_{yz}\end{aligned} \tag{8}$$

$C_{ij}$ can be expressed as follows:

$$\frac{E}{1-\nu^2} = C_{11} = C_{22}, \frac{\nu E}{1-\nu^2} = C_{12}, \frac{E}{2(1+\nu)} = C_{44} = C_{55} = C_{66} \tag{9}$$

## *Equations of motion*

The isotropic plate considered in this study rests on a homogeneous viscoelastic foundation that is defined by three parameters, namely, the linear Winkler modulus Kw, Pasternak shear modulus Ks, and damping coefficient of the viscoelastic medium Ct.

In the case of an unglued contact, i.e. when there is no adhesion, between the isotropic plate and the support, the interaction follows the three-parameter visco-Pasternak foundation model, similar to that established by Zenkour (2016).

It is noteworthy that the vertical reaction $R_f$ of the viscoelastic foundation is expressed as:

$$R_f = \left(k_w - k_s\nabla^2 + C_t\frac{\partial}{\partial t}\right)w \tag{10}$$

On the other hand, the Hamilton's principle is employed to derive the equations of motion. Hence:

$$0 = \int_0^t \left(\delta U + \delta V - \delta K + \delta R_f\right)dt \tag{11}$$

Here, $\delta U$ denotes the strain energy variation, $\delta V$ the potential energy variation, and $\delta K$ the kinetic energy variation.

The above strain energy variation for an isotropic plate may be written as:

$$\delta U = \int_V \left[\sigma_x \delta\varepsilon_x + \sigma_y \delta\varepsilon_y + \tau_{xy}\delta\gamma_{xy} + \tau_{yz}\delta\gamma_{yz} + \tau_{xz}\delta\gamma_{xz}\right] dV$$

$$= \int_A \left[M_x \delta k_x^b + M_y \delta k_y^b + M_{xy}\delta k_{xy}^b + N_{sx}\delta k_x^s + N_{sy}\delta k_y^s + N_{sxy}\delta k_{xy}^s + N_{Tcx}\delta\gamma_{xz}^0 + N_{Tcy}\delta\gamma_{yz}^0\right] dV \quad (12)$$

where A is the top surface. The stress resultants M and N are given by:

$$\left(M_x, M_y, M_{xy}\right) = \int_{-h/2}^{h/2} \left(\sigma_x, \sigma_y, \tau_{xy}\right) z dz \ , \left(N_{sx}, N_{sy}, N_{sxy}\right)$$

$$= \int_{-h/2}^{h/2} \left(\sigma_x, \sigma_y, \tau_{xy}\right) f(z) dz \quad (13)$$

$$\text{and } \left(N_{Tcx}, N_{Tcy},\right) = \int_{-h/2}^{h/2} \left(\tau_{xz}, \tau_{yz}\right) g(z) dz$$

Likewise, the variation of external work can be written as:

$$\delta V = -\int_A q \delta w_0 dA \quad (14)$$

Similarly, the variation of kinetic energy of the plate is given by:

$$\delta K = \int_V \left(\ddot{u}\ \delta u + \ddot{v}\ \delta v + \ddot{w}\ \delta w\right) \rho dV$$

$$\delta K = \int_A \left\{ I_1 \ddot{w}_0 \partial w_0 + I_2 \left(\frac{\partial \ddot{w}_0}{\partial x}\frac{\partial \delta w_0}{\partial x} + \frac{\partial \ddot{w}_0}{\partial y}\frac{\partial \delta w_0}{\partial y}\right) - I_3 - I_3\left(K_1 \acute{A}\frac{\partial \ddot{w}_0}{\partial x}\frac{\partial \delta\theta}{\partial x} + K_1\acute{A}\frac{\partial \ddot{\theta}}{\partial x}\frac{\partial \delta w_0}{\partial x} + K_2\acute{B}\frac{\partial \ddot{w}_0}{\partial y}\frac{\partial \delta\theta}{\partial y} + K_2\acute{B}\frac{\partial \ddot{\theta}}{\partial y}\frac{\partial \delta w_0}{\partial y}\right) + I_4\left(\left(K_1\acute{A}\right)^2\frac{\partial \ddot{\theta}}{\partial x}\frac{\partial \delta\theta}{\partial x} + \left(K_2\acute{B}\right)^2\frac{\partial \ddot{\theta}}{\partial y}\frac{\partial \delta\theta}{\partial y}\right)\right\} dA \quad (15)$$

The dot superscript indicates differentiation with respect to time t, $\rho$ is the mass density, and $I_i$ denotes the mass inertias, as expressed below:

$$(I_1, I_2, I_3, I_4) = \int_{-h/2}^{h/2} (1, z^2, zf(z), f(z)^2)\rho dz \tag{16}$$

Substitution of Eqs. (12), (14) and (15) into Eq. (11) leads to the following equations of motion:

$$\begin{aligned}
\delta w_0: & -\frac{\partial^2 M_x}{\partial x^2} - \frac{\partial^2 M_y}{\partial y^2} - 2\frac{\partial^2 M_{xy}}{\partial x \partial y} + q + k_w w_0 - k_s^x \frac{\partial^2 w_0}{\partial x^2} - k_s^y \frac{\partial^2 w_0}{\partial y^2} \\
& + k_w + c_t * \frac{\partial w_0}{\partial t} \\
= & -I_1 \frac{\partial^2 w_0}{\partial t^2} + I_2 \left( \frac{\partial^4 w_0}{\partial x^2 \partial t^2} + \frac{\partial^4 w_0}{\partial y^2 \partial t^2} \right) \\
& - I_3 \left( K_1 \acute{A} \frac{\partial^4 \theta}{\partial x^2 \partial t^2} + K_2 \acute{B} \frac{\partial^4 \theta}{\partial y^2 \partial t^2} \right) \\
\delta \theta: & K_1 \acute{A} \frac{\partial^2 N_{sx}}{\partial x^2} + K_2 \acute{B} \frac{\partial^2 N_{sy}}{\partial y^2} + \left( K_1 \acute{A} + K_2 \acute{B} \right) \frac{\partial^2 N_{sxy}}{\partial x \partial y} - K_1 \acute{A} \frac{\partial N_{Tcx}}{\partial x} \\
& - K_2 \acute{B} \frac{\partial N_{Tcy}}{\partial y} \\
= & -I_3 \left( K_1 \acute{A} \frac{\partial^4 w_0}{\partial x^2 \partial t^2} + \quad K_2 \acute{B} \frac{\partial^4 w_0}{\partial y^2 \partial t^2} \right) \\
& + I_4 \left( \left( K_1 \acute{A} \right)^2 \frac{\partial^4 \theta}{\partial x^2 \partial t^2} + \left( K_2 \acute{B} \right)^2 \frac{\partial^4 \theta}{\partial y^2 \partial t^2} \right)
\end{aligned} \tag{17}$$

Similarly, substituting Eq. (4) into Eq. (8) and incorporating the resulting expressions into Eqs. (13) allows deriving the equations of motion in terms of displacements, in the following compact form:

$$\begin{Bmatrix} M \\ N_S \end{Bmatrix} = \begin{Bmatrix} A & B \\ B & A_s \end{Bmatrix} \begin{Bmatrix} k^b \\ k^s \end{Bmatrix}, \; N_{Tc} = H\gamma \tag{18}$$

in which

$$\begin{gathered}
M = \left\{ M_x, M_y, M_{xy} \right\}^t, N_s = \left\{ N_{sx}, N_{sy}, N_{sxy} \right\}^t \\
k^b = \left\{ k_x^b, k_y^b, k_{xy}^b \right\}^t, k^s = \left\{ k_x^s, k_y^s, k_{xy}^s \right\}^t
\end{gathered} \tag{19}$$

$$\begin{gathered}
\text{with } A = \begin{bmatrix} A_{11} & A_{12} & 0 \\ A_{12} & A_{22} & 0 \\ 0 & 0 & A_{66} \end{bmatrix}, B = \begin{bmatrix} B_{11} & B_{12} & 0 \\ B_{12} & B_{22} & 0 \\ 0 & 0 & B_{66} \end{bmatrix}, \\
A_s = \begin{bmatrix} A_{s11} & A_{s12} & 0 \\ A_{s12} & A_{s22} & 0 \\ 0 & 0 & A_{s66} \end{bmatrix}
\end{gathered} \tag{20}$$

$$N_{Tc} = \{N_{Tcx}, N_{Tcy}\}^t, \gamma = \{\gamma_{xz}^0, \gamma_{yz}^0\}^t,$$
$$H = \begin{bmatrix} H_{44} & 0 \\ 0 & H_{55} \end{bmatrix}$$

Likewise, the stiffness components are defined as follows:

$$\left(A_{ij}, B_{ij}, A_{sij}\right) = \int_{-h/2}^{h/2} (z^2, zf(z), f(z)^2) C_{ij} dz \ , (i,j = 1,2,6)$$
$$H_{ij} = \int_{-h/2}^{h/2} \acute{f}(z)^2 C_{ij} dz \ , (i,j = 4,5) \quad (21)$$

Thus, substituting Eq. (18) into Eq. (17) allows formulating the equations of motion in terms of displacements $(w_0, \theta)$. The resulting governing equations may then be written in the following form:

$$\begin{aligned}
&A_{11}d_{1111}w_0 - B_{11}K_1\acute{A}d_{1111}\theta + 2A_{12}d_{1122}w_0 \\
&\quad - B_{12}\left(K_1\acute{A} + K_2\acute{B}\right)d_{1122}\theta + A_{22}d_{2222}w_0 \\
&\quad - \ B_{22}K_2\acute{B}d_{2222}\theta + 4A_{66}d_{1122}w_0 \\
&\quad - 2B_{66}\left(K_1\acute{A} + K_2\acute{B}\right)d_{1122}\theta + q + k_w w_0 - k_s^x d_{11}w_0 \\
&\quad - k_s^y d_{22}w_0 + c_t * \dot{w}_0 \\
&\quad = -I_1\ddot{w}_0 + I_2(d_{11}\ddot{w}_0 + \ d_{22}\ddot{w}_0) \\
&\quad - \ I_3\left(K_1\acute{A}d_{11}\ddot{\theta} + K_2\acute{B}d_{22}\ddot{\theta}\right) \\
&\left(-B_{11}d_{1111}w_0 + A_{s11}K_1\acute{A}d_{1111}\theta - B_{12}d_{1122}w_0\right. \\
&\quad \left. + A_{s12}K_2\acute{B}d_{1122}\theta\right)K_1\acute{A} \\
&\quad + \left(-B_{12}d_{1122}w_0 + \ A_{s12}K_1\acute{A}d_{1122}\theta - B_{22}d_{2222}w_0\right. \\
&\quad \left. + A_{s22}K_2\acute{B}d_{2222}\theta\right)K_2\acute{B} \\
&\quad + \left(-2B_{66}d_{1122}w_0\right. \\
&\quad \left. + A_{s66}\left(K_1\acute{A} + \ K_2\acute{B}\right)d_{1122}\theta\right)\left(K_1\acute{A} + K_2\acute{B}\right) \\
&\quad - \left(K_1\acute{A}\right)^2 H_{55}d_{11}\theta - \left(K_2\acute{B}\right)^2 H_{44}d_{22}\theta \\
&\quad = -I_3\left(K_1\acute{A}d_{11}\ddot{w}_0 + \ K_2\acute{B}d_{22}\ddot{w}_0\right) \\
&\quad + I_4\left(\left(K_1\acute{A}\right)^2 d_{11}\ddot{\theta} + \left(K_2\acute{B}\right)^2 d_{22}\ddot{\theta}\right)
\end{aligned} \quad (22)$$

where $d_{ij}, d_{ijl}$ and $d_{ijlm}$ represent the following differential operators:

$$d_{ij} = \frac{\partial^2}{\partial x_i \partial x_j}, d_{ijl} = \frac{\partial^3}{\partial x_i \partial x_j \partial x_l}, d_{ijlm} = \frac{\partial^4}{\partial x_i \partial x_j \partial x_l \partial x_m}, d_i = \frac{\partial}{\partial x_i}, \quad (i,j,l,m = 1,2) \quad (23)$$

Regarding the shear stresses $(\tau_{xz}, \tau_{yz})$, they can be expressed either by the constitutive relations in Eq. (8), or by integrating the 3D elasticity equilibrium equations with respect to the thickness coordinate, as previously reported by Younsi et al. (2018) and Boulefrakh et al. (2019).

$$\frac{\partial \sigma_x}{\partial x}+\frac{\partial \tau_{xy}}{\partial y}+\frac{\partial \tau_{xz}}{\partial z}=0 \text{ and } \frac{\partial \tau_{xy}}{\partial x}+\frac{\partial \sigma_y}{\partial y}+\frac{\partial \tau_{yz}}{\partial z}=0 \quad (24)$$

Then, integrating Eq. (24) with respect to the thickness coordinate z, and applying appropriate boundary conditions at the upper and lower surfaces of the plate, yields:

$$[\tau_{xz}]_{z=\pm h/2}=0\,, \qquad [\tau_{yz}]_{z=\pm h/2}=0 \quad (25)$$

It is important to note that, in this study, $\tau_{xz}^{CR}$ and $\tau_{yz}^{CR}$ are the stresses obtained by the constitutive relations, while $(\tau_{xz}^{EE}, \tau_{yz}^{EE})$ are the stresses calculated using the equilibrium equations.

### *Analytical solution for simply-supported FG plates*

The analytical Navier solution method is adopted to obtain analytical solutions in which the displacement components are represented by the product of arbitrary parameters and some known trigonometric functions. This approach ensures that the governing equations of motion and the associated boundary conditions are both satisfied.

$$\begin{Bmatrix} w_0 \\ \theta \end{Bmatrix}=\sum_{m=1}^{\infty}\sum_{n=1}^{\infty}\begin{Bmatrix} w_{mn}e^{i\omega t}sin(\lambda x)sin(\mu y) \\ \theta_{mn}e^{i\omega t}sin(\lambda x)sin(\mu y) \end{Bmatrix} \quad (26)$$

Here, $\omega$ is the frequency of the plate's free vibration, and $\sqrt{i}=-1$ represents the imaginary unit.

with

$$\lambda=\frac{m\pi}{a} \quad , \qquad \mu=\frac{n\pi}{b} \quad (27)$$

The transverse load q is expanded in the double-Fourier sine series as:

- Bending analysis of isotropic plates subjected to a uniformly distributed load:

$$q(x,y)=\sum_{m=1}^{\infty}\sum_{n=1}^{\infty}q_{mn}sin\left(\frac{m\pi}{a}x\right)sin\left(\frac{n\pi}{b}y\right) \quad (28)$$

where

$$q_{mn}=\frac{16q_0}{mn\pi^2}\ for\ m=1,3,5,\ldots\ldots and\ \ n=1,3,5,\ldots.$$

$$q_{mn}=0\ \ for\ m=2,4,4,\ldots\ldots and\ \ n=2,4,4,\ldots\ldots$$

-Bending analysis of isotropic plates subjected to a sinusoidally distributed load:

$$q(x,y)=q_0sin\left(\frac{\pi}{a}x\right)sin\left(\frac{n\pi}{b}y\right) \quad (29)$$

Substitution of Eq. (26) into Eq. (22) leads to the following analytical solution:

$$\left(\begin{bmatrix} K_{11} & K_{12} \\ K_{12} & K_{22} \end{bmatrix} - \omega^2 \begin{bmatrix} m_{11} & m_{12} \\ m_{12} & m_{22} \end{bmatrix}\right)\begin{Bmatrix} w_{mn} \\ \theta_{mn} \end{Bmatrix} = \begin{Bmatrix} q_{mn} \\ 0 \end{Bmatrix} \tag{30}$$

where

$$\begin{aligned}
K_{11} &= 2(2A_{66} + A_{12})\lambda^2\mu^2 + A_{22}\mu^4 + A_{11}\lambda^4 + k_s^x\lambda^2 + k_s^y\mu^2 + k_w \\
&\quad - c_t * \omega \\
K_{12} &= -2\left(K_1\acute{A} + K_2\acute{B}\right)B_{66}\lambda^2\mu^2 - \left(K_1\acute{A} + K_2\acute{B}\right)B_{12}\lambda^2\mu^2 \\
&\quad - K_1\acute{A}B_{11}\lambda^4 - K_2\acute{B}B_{22}\mu^4 \\
K_{22} &= \left(K_1\acute{A}\lambda^4 A_{s11} + K_2\acute{B}\lambda^2\mu^2 A_{s12}\right)K_1\acute{A} + \left(K_1\acute{A}\right)^2\lambda^2 H_{55} \\
&\quad + \left(K_1\acute{A}\lambda^2\mu^2 A_{s12} + K_2\acute{B}\mu^4 A_{s22}\right)K_2\acute{B} \\
&\quad + \left(K_2\acute{B}\right)^2\mu^2 H_{44} \\
&\quad + \left(K_1\acute{A}\lambda^2\mu^2 A_{s66} + K_2\acute{B}\lambda^2\mu^2 A_{s66}\right)\left(K_1\acute{A} + K_2\acute{B}\right) \\
m_{11} &= I_1 + I_2(\lambda^2 + \mu^2) \\
m_{12} &= -I_3\left(K_1\acute{A}\lambda^2 + K_2\acute{B}\mu^2\right) \\
m_{22} &= I_4\left(\left(K_1\acute{A}\right)^2\lambda^2 + \left(K_2\acute{B}\right)^2\mu^2\right)
\end{aligned} \tag{31}$$

## Numerical results and discussion

Various numerical examples are provided and discussed in prder to demonstrate the effect of the visco-Pasternak foundation on the bending and free vibration responses of simply supported thick isotropic square and rectangular plates.

Then, the results obtained by means of the present high-order shear deformation theory (HSDT) are compared with those derived from other well-established HSDTs, including those proposed by Reddy (1984), Ghugal and Sayyad (2010), Ghugal and Pawar (2011), Sayyad and Ghugal (2012), and Djidar et al. (2022). Moreover, some additional comparisons are made with the predictions of the first-order shear deformation theory (FSDT) previously developed by Mindlin (1951), the classical plate theory (CPT) of Kirchhoff (1850), and the exact elasticity solution of Pagano (1970).

For the sake of consistency, the numerical results related to bending and free vibration are presented in a non-dimensional form, using the following relations:

$$\begin{aligned}
&\bar{u} = \frac{uE_2}{qhS^3}, \bar{w} = \frac{100Ew}{qhS^4}, \left(\bar{\sigma}_x, \bar{\sigma}_y\right) = \frac{\left(\sigma_x, \sigma_y\right)}{qS^2}, \bar{\tau}_{zx} = \frac{\tau_{xz}}{qS}, \\
&\bar{\omega} = \omega_{mn}h\sqrt{\rho/G}, \quad \bar{c}_t = \frac{a^4 c_t}{10^3 D_c}, \qquad K_w = \frac{k_w a^4}{h^3}, \quad K_s = \frac{k_s a^2}{h^3 v}
\end{aligned} \tag{32}$$

where S (a/h) represents the thickness ratio.

The properties of the isotropic plate material are:

$$E = 210GPa, \qquad v = 0.3, \qquad G = \frac{E}{2(1+v)} \text{ and } \rho = 7800\,Kg/m^3$$

where E is Young's modulus, G is the shear modulus, $v$ is Poisson's ratio and ρ is the material's density.

### *Bending analysis*

In the first example, the displacements and stresses for the isotropic square plate simply supported on a viscoelastic foundation and subjected to a uniformly distributed load for both aspect ratios *(a/h)*, i.e. 4 and 10, are compared in Table 1 with those previously published. It can be readily observed that when the viscosity term $\bar{C}_t$ and elastic foundation parameters $K_w$, $K_S$ are omitted, good agreement between the results is then obtained. It may also be noted that the displacements and stresses decrease with the incorporation of the viscoelastic foundation parameters. Moreover, when the visco-Winkler-Pasternak foundation parameters $\bar{C}_t$ ,$K_w$ and $K_S$increase, the displacements and stresses decrease. However, it is important to emphasize that the effect of the Pasternak shear modulus parameter ($K_s$) is more significant than that of Winkler modulus parameter $K_w$.

In the second example, Table 2 presents a comparison between the displacements and stresses obtained using the proposed theory and others reported in the literature. The results are provided for the isotropic square plate simply supported on a viscoelastic foundation and subjected to a sinusoidally distributed load for different values of $K_w$, $K_S$ and $\bar{C}_t$. It turns out that in the case where the damping coefficient $\bar{C}_t$ and elastic foundation parameters $K_w$ and $K_S$ are equal to zero, the different theories are in excellent agreement. It was also found that using visco-Winkler-Pasternak foundations leads to smaller displacements and stresses.

Furthermore, it was revealed that high values of the elastic foundation modulus and damping coefficient enhance the bending rigidity of the isotropic plate.

*Table 1 – Comparison of non-dimensional in-plane displacement* $(\bar{u})$ *at* $(x = 0,\ y = b/2, z = \pm h/2)$*, transverse displacement* $(\bar{w})(x = a/2, y = b/2, z = 0)$*, in-plane normal stress* $(\bar{\sigma}_x)(x = a/2, y = b/2, z = \pm h/2)$*, in-plane shear stress* $(\bar{\sigma}_{xy})(x = 0, y = 0, z = \pm h/2)$*, and transverse shear stress* $(\bar{\sigma}_{zx})(x = 0, y = b/2, z = 0)$ *in an isotropic square plate subjected to a uniformly distributed load*

| S | Theory | Model | $K_w$ | $K_s$ | $\bar{C}_t$ | $\bar{u}$ | $\bar{w}$ | $\bar{\sigma}_x$ | $\bar{\sigma}_{xy}$ | $\bar{\tau}_{zx}^{EE}$ |
|---|---|---|---|---|---|---|---|---|---|---|
| | A.S.Sayyad (2012) | ESDT | | | | 0.079 | 5.816 | 0.3 | 0.223 | 0.472 |
| | Reddy (1984) | HSDT | | | | 0.079 | 5.869 | 0.299 | 0.218 | 0.452 |
| | Ghugal & Sayyad (2011) | TSDT | | | | 0.074 | 5.68 | 0.318 | 0.208 | 0.42 |
| | Ghugal & Pawar (2011) | HPSDT | 0 | 0 | 0 | 0.079 | 5.858 | 0.297 | 0.185 | 0.451 |
| | Mindlin (1951) | FSDT | | | | 0.074 | 5.633 | 0.287 | 0.195 | 0.495 |
| | Kirchhoff (1850) | CPT | | | | 0.074 | 4.436 | 0.287 | 0.195 | 0.495 |
| | Pagano (1970) | Elasticity | | | | 0.072 | 5.694 | 0.307 | – | – |
| | Djidar et al. (2022) | ESDT | | | | 0.079 | 5.858 | 0.300 | 0.223 | 0.4504 |
| 4 | Present | ESDT | 0 | 0 | 0 | **0.079** | **5.858** | **0.300** | **0.223** | **0.4504** |
| | | | 5 | 0 | 0.01 | **0.077** | **5.654** | **0.289** | **0.218** | **0.4375** |
| | | | | | 0.05 | **0.072** | **5.284** | **0.269** | **0.206** | **0.414** |
| | | | | | 0.1 | **0.067** | **4.883** | **0.246** | **0.194** | **0.389** |
| | | | 0 | 5 | 0.01 | **0.059** | **4.274** | **0.215** | **0.172** | **0.342** |
| | | | | | 0.05 | **0.056** | **4.057** | **0.2035** | **0.165** | **0.329** |
| | | | | | 0.1 | **0.053** | **3.814** | **0.190** | **0.157** | **0.313** |
| | | | 5 | 5 | 0.01 | **0.058** | **4.218** | **0.212** | **0.170** | **0.339** |
| | | | | | 0.05 | **0.056** | **4.006** | **0.201** | **0.163** | **0.325** |
| | | | | | 0.1 | **0.053** | **3.768** | **0.188** | **0.156** | **0.310** |
| | A.S.Sayyad (2012) | ESDT | | | | 0.075 | 4.658 | 0.289 | 0.204 | 0.49 |
| | Reddy (1984) | HSDT | | | | 0.075 | 4.666 | 0.289 | 0.203 | 0.486 |
| | Ghugal & Sayyad (2011) | TSDT | | | | 0.073 | 4.625 | 0.307 | 0.195 | 0.481 |
| | Ghugal & Pawar (2011) | HPSDT | 0 | 0 | 0 | 0.074 | 4.665 | 0.289 | 0.193 | 0.486 |
| | Mindlin (1951) | FSDT | | | | 0.074 | 4.67 | 0.287 | 0.195 | 0.495 |
| | Kirchhoff (1850) | CPT | | | | 0.074 | 4.436 | 0.287 | 0.195 | 0.495 |
| | Pagano (1970) | Elasticity | | | | 0.073 | 4.639 | 0.289 | – | – |
| | Djidar et al (2022) | ESDT | | | | 0.074 | 4.664 | 0.289 | 0.200 | 0.484 |
| 10 | Present | ESDT | 0 | 0 | 0 | **0.074** | **4.664** | **0.289** | **0.200** | **0.484** |
| | | | 5 | 0 | 0.01 | **0.073** | **4.538** | **0.281** | **0.196** | **0.474** |
| | | | | | 0.05 | **0.069** | **4.304** | **0.265** | **0.187** | **0.455** |
| | | | | | 0.1 | **0.065** | **4.043** | **0.248** | **0.178** | **0.434** |
| | | | 0 | 5 | 0.01 | **0.059** | **3.6205** | **0.221** | **0.161** | **0.395** |
| | | | | | 0.05 | **0.056** | **3.469** | **0.2105** | **0.1555** | **0.383** |
| | | | | | 0.1 | **0.054** | **3.296** | **0.199** | **0.149** | **0.369** |
| | | | 5 | 5 | 0.01 | **0.058** | **3.581** | **0.218** | **0.160** | **0.392** |
| | | | | | 0.05 | **0.056** | **3.433** | **0.208** | **0.154** | **0.380** |
| | | | | | 0.1 | **0.053** | **3.263** | **0.197** | **0.148** | **0.366** |

*Table 2 – Comparison of non-dimensional in-plane displacement* $(\bar{u})$ *at* $(x = 0, y = b/2, z = \pm h/2)$*, transverse displacement* $(\bar{w})$ *at* $(x = a/2, y = b/2, z = 0)$*, in-plane normal stress* $(\bar{\sigma}_x)$ *at* $(x = a/2, y = b/2, z = \pm h/2)$*, in-plane shear stress* $(\bar{\sigma}_{xy})$ *at* $(x = 0, y = 0, z = \pm h/2)$ *and transverse shear stress* $(\bar{\sigma}_{zx})$ *at* $(x = 0, y = b/2, z = 0)$ *in an isotropic square plate subjected to a sinusoidal load.*

| S | Theory | Model | $K_w$ | $K_s$ | $\bar{C}_t$ | $\bar{u}$ | $\bar{w}$ | $\bar{\sigma}_x$ | $\bar{\sigma}_{xy}$ | $\bar{\tau}_{zx}^{EE}$ |
|---|---|---|---|---|---|---|---|---|---|---|
| 4 | A.S.Sayyad (2012) | ESDT | 0 | 0 | 0 | 0.046 | 3.748 | 0.213 | 0.114 | 0.236 |
| | Reddy (1984) | HSDT | | | | 0.046 | 3.787 | 0.209 | 0.112 | 0.226 |
| | Ghugal & Sayyad (2011) | TSDT | | | | 0.044 | 3.653 | 0.226 | 0.133 | 0.232 |
| | Ghugal & Pawar (2011) | HPSDT | | | | 0.047 | 3.779 | 0.209 | 0.112 | 0.235 |
| | Mindlin (1951) | FSDT | | | | 0.044 | 3.626 | 0.197 | 0.106 | 0.239 |
| | Kirchhoff (1850) | CPT | | | | 0.044 | 2.803 | 0.197 | 0.106 | 0.238 |
| | Pagano (1970) | Elasticity | | | | 0.049 | 3.662 | 0.217 | – | – |
| | Djidar et al. (2022) | ESDT | | | | 0.046 | 3.778 | 0.21 | 0.113 | 0.234 |
| | Present | ESDT | 0 | 0 | 0 | **0.046** | **3.778** | **0.21** | **0.113** | **0.234** |
| | | | 5 | 0 | 0.01 | **0.045** | **3.652** | **0.203** | **0.110** | **0.226** |
| | | | | | 0.05 | **0.042** | **3.423** | **0.191** | **0.103** | **0.212** |
| | | | | | 0.1 | **0.039** | **3.174** | **0.177** | **0.095** | **0.197** |
| | | | 0 | 5 | 0.01 | **0.035** | **2.781** | **0.155** | **0.083** | **0.172** |
| | | | | | 0.05 | **0.033** | **2.646** | **0.147** | **0.079** | **0.164** |
| | | | | | 0.1 | **0.031** | **2.495** | **0.139** | **0.075** | **0.155** |
| | | | 5 | 5 | 0.01 | **0.034** | **2.746** | **0.153** | **0.082** | **0.170** |
| | | | | | 0.05 | **0.032** | **2.614** | **0.146** | **0.078** | **0.162** |
| | | | | | 0.1 | **0.031** | **2.467** | **0.137** | **0.074** | **0.153** |
| 10 | A.S.Sayyad (2012) | ESDT | 0 | 0 | 0 | 0.044 | 2.954 | 0.2 | 0.108 | 0.238 |
| | Reddy (1984) | HSDT | | | | 0.044 | 2.961 | 0.199 | 0.107 | 0.229 |
| | Ghugal & Sayyad (2011) | TSDT | | | | 0.044 | 2.933 | 0.212 | 0.11 | 0.235 |
| | Ghugal & Pawar (2011) | HPSDT | | | | 0.044 | 2.959 | 0.199 | 0.107 | 0.238 |
| | Mindlin (1951) | FSDT | | | | 0.044 | 2.934 | 0.197 | 0.106 | 0.239 |
| | Kirchhoff (1850) | CPT | | | | 0.044 | 2.802 | 0.197 | 0.106 | 0.238 |
| | Pagano (1970) | Elasticity | | | | 0.044 | 2.942 | 0.2 | – | – |
| | Djidar et al. (2022) | ESDT | | | | 0.044 | 2.959 | 0.200 | 0.108 | 0.238 |
| | Present | ESDT | 0 | 0 | 0 | **0.044** | **2.959** | **0.200** | **0.108** | **0.238** |
| | | | 5 | 0 | 0.01 | **0.043** | **2.881** | **0.194** | **0.105** | **0.232** |
| | | | | | 0.05 | **0.041** | **2.737** | **0.185** | **0.099** | **0.220** |
| | | | | | 0.1 | **0.039** | **2.576** | **0.174** | **0.094** | **0.207** |
| | | | 0 | 5 | 0.01 | **0.035** | **2.310** | **0.156** | **0.084** | **0.186** |
| | | | | | 0.05 | **0.033** | **2.217** | **0.150** | **0.081** | **0.178** |
| | | | | | 0.1 | **0.032** | **2.109** | **0.142** | **0.077** | **0.170** |
| | | | 5 | 5 | 0.01 | **0.034** | **2.286** | **0.154** | **0.083** | **0.184** |
| | | | | | 0.05 | **0.033** | **2.194** | **0.148** | **0.080** | **0.176** |
| | | | | | 0.1 | **0.031** | **2.089** | **0.141** | **0.076** | **0.168** |

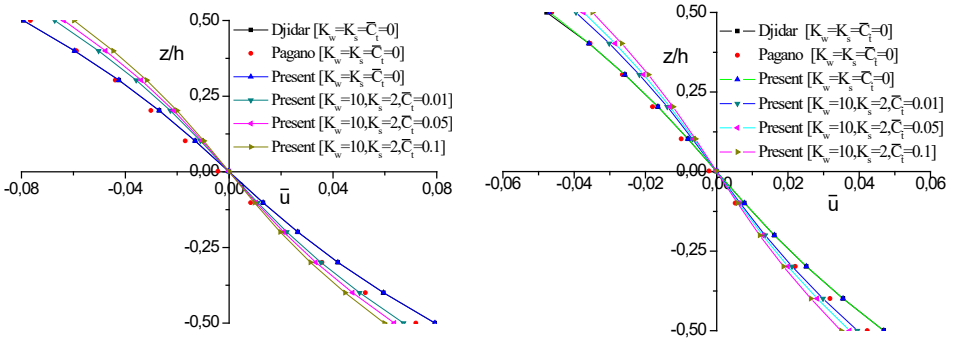



*Figure 2 – Variation of the in-plane displacement as a function of the thickness of an isotropic plate subjected successively to a uniformly distributed load and a single sinusoidal load for different values of $\bar{C}_t$ , $K_w$ and $K_s$ (a/h= 4)*

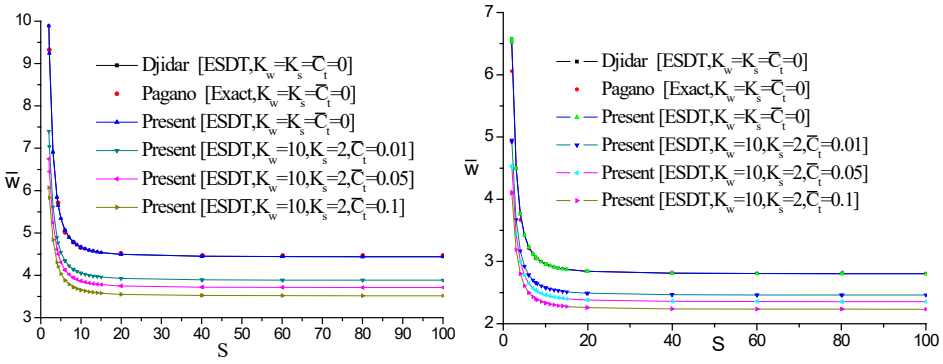



Figure 3 – Variation of the transverse displacement as a function of the thickness of an isotropic plate subjected successively to a uniformly distributed load and a single sinusoidal load for different values of $\bar{C}_t$, $K_w$ and $K_s$

Figure 2 presents the in-plane displacement $\bar{u}$ through the thickness of the isotropic plate subjected to a uniformly distributed load (UDL) and a sinusoidally distributed load (SDL), successively, for different values of the viscosity term $\bar{C}_t$ and elastic foundation parameters $K_w$ and $K_S$. This figure clearly indicates that increasing $\bar{C}_t$, $K_w$, and $K_S$ induces a reduction in the in-plane displacement of the isotropic plate. Furthermore, the plots in this same figure also show that the $\bar{u}$ values obtained with the method proposed in this work, in which the effect of viscoelastic foundation parameters is taken into account, are smaller than those previously found

by Djidar et al. and Pagano, who had neglected the parameters $K_w$, $K_S$ and $\bar{C}_t$.

Figure 3 displays the variations of the transverse displacement $\bar{w}$ of the isotropic plate subjected to a UDL and a SDL, successively, versus the aspect ratio (a/h), for different values of $K_w$, $K_S$ and $\bar{C}_t$. It is clearly shown that the transverse displacement $\bar{w}$ decreases as the aspect ratio (a/h) increases. Moreover, the resulting curves suggest that the presence of viscoelastic foundations leads to a decline in the transverse displacement $\bar{w}$ of the isotropic plate. In addition, it is also observed, as expected, that the results obtained indicate that the Pagano and Djidar models generate larger transverse displacements, as these two models do not take into account the effects of the parameters $K_w$, $K_S$ and $\bar{C}_t$.

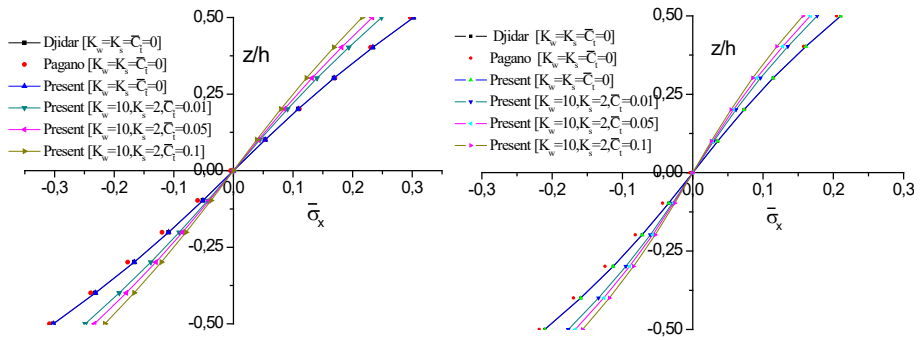



*Figure 4 – Variation of the in-plane normal stress as a function of the thickness of an isotropic plate subjected successively to a uniformly distributed load and a single sinusoidal load for different values of $\bar{C}_t$ , $K_w$ and $K_s$ (a/h= 4)*

Figure 4 depicts the graphical variations of the in-plane normal stresses $\bar{\sigma}_x$ across the thickness of the isotropic plate, successively under UDL and SDL, for different values of the damping coefficient $\bar{C}_t$ and elastic foundation parameters $K_w$ and $K_S$. This figure explicitly indicates that the maximum tensile stresses occur at a point near the bottom surface of the isotropic plate, while the maximum compressive stresses occur at a point near the upper surface. In addition, the curves in this figure suggest that the visco-elastic foundation has a significant impact on the in-plane normal stress values.

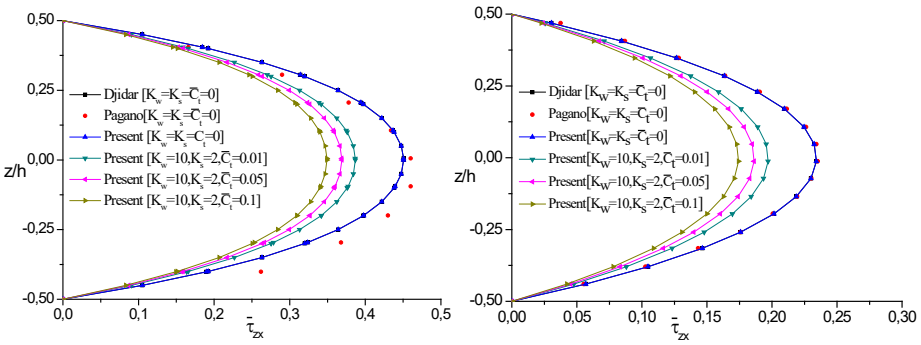



*Figure 5 – Variation of the transverse shear stress as a function of the thickness through an isotropic plate subjected successively to a uniformly distributed load and a single sinusoidal load for different values of $\bar{C}_t$, $K_w$ and $K_s$ (a/h= 4)*

Figure 5 depicts the through-the-thickness distributions of transverse shear stresses within the square isotropic plate, successively under UDL and SDL. The aspect ratio (a/h) is taken as equal to 4. It is clearly established that the zero shear stress condition at the upper and lower faces of the plate is fully satisfied. It is also observed that the transverse shear stress increases gradually as the $\bar{C}_t$, $K_w$ and $K_S$ values decrease. It can therefore be inferred that the introduction of large visco-elastic foundation parameters can enhance the bending rigidity of the isotropic plate.

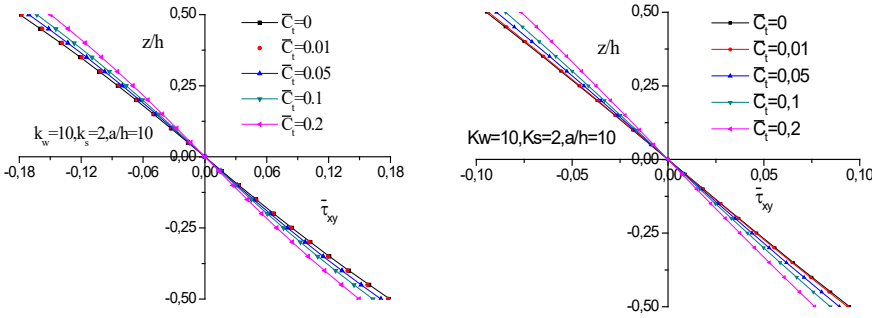



*Figure 6 – Variation of the in-plane shear stress as a function of the thickness across an isotropic plate, successively subjected to a uniformly distributed load and a single sinusoidal load for different values of $\bar{C}_t$ (a/h = 10, $K_w = 10$ and, $K_s = 2$) (a/h = 10, $K_w = 10$ and, $K_s = 2$)*

Figure 6 presents the variations of the in-plane shear stresses $\bar{\tau}_{xy}$ through the thickness of the isotropic plate, successively subjected to UDL

and SDL, for different values of the viscosity term $\bar{C}_t$. The results obtained reveal that the in-plane compressive and tensile shear stress values are maximum at points near the top and bottom surfaces of the isotropic plate, respectively.

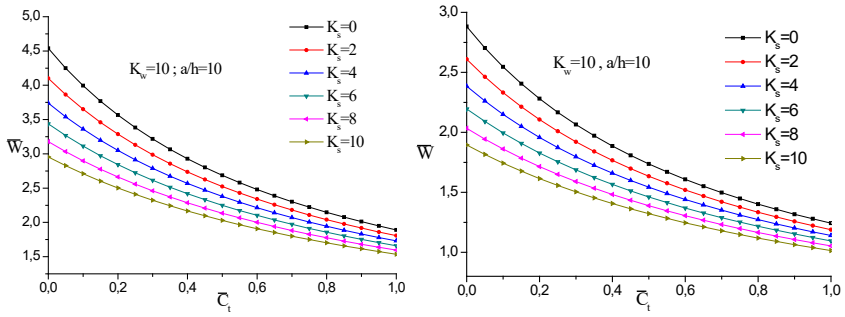



*Figure 7 – Effect of damping coefficient and Pasternak shear modulus parameter on the transverse displacement of an isotropic plate, successively subjected to uniformly distributed load and single sine load for different values of $K_s$ (a/h = 10, $K_w = 10$)*

Figure 7 presents the variation of the transverse displacement $\bar{w}$ of the isotropic plate successively subjected to a uniformly distributed load and a single sine load versus the damping coefficient $\bar{C}_t$ for various values of the Pasternak shear modulus parameter $K_S$. It is clearly observed that when the viscosity term is taken into account, the transverse displacement $\bar{w}$ declines due to the damping effect. This same figure also shows that when the parameter $K_S$ increases, the transverse displacement of the isotropic plate diminishes.

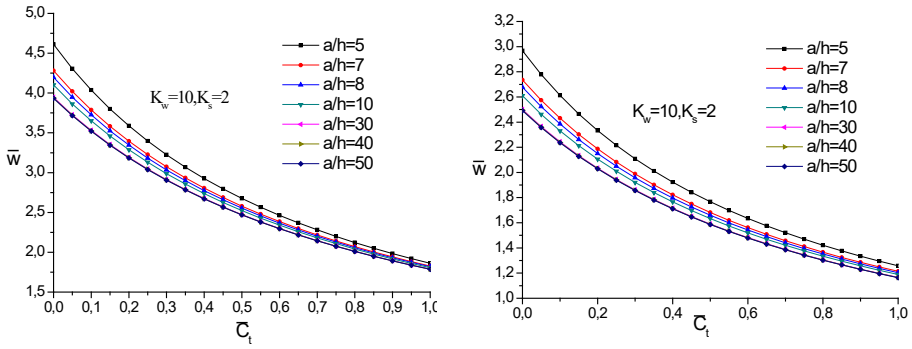



*Figure 8 – Effect of damping coefficient on the transverse displacement of the isotropic plate, successively subjected to uniformly distributed load and single sine load for different values of a/h ($K_w = 10$, $K_s = 2$)*

Likewise, Figure 8 illustrates the variation of the transverse

displacement $\overline{w}$ of the isotropic plate, successively subjected to UDL and SDL, as a function of the damping coefficient $\bar{C}_t$ for various aspect ratios (a/h). This figure also indicates that the transverse displacement $\overline{w}$ diminishes as the aspect ratio (a/h) rises. It should be emphasized that increasing the damping coefficient leads to a more rigid plate.

## *Vibration analysis*

In this section, two numerical examples are presented and discussed to assess the accuracy of the proposed theory in predicting the dynamic response of plates.

*Table 3 – Comparison between natural bending mode frequencies* $(\bar{\omega}_w)$ *and thickness shear mode frequencies* $(\bar{\omega}_\theta)$ *for simply supported isotropic square plates* $(S = 10)$.

| a/b | w | Theory | Kw | Ks | $\bar{C}_t$ | (m.n) | | | | | | |
|---|---|---|---|---|---|---|---|---|---|---|---|---|
| | | | | | | 1.1 | 1.2 | 1.3 | 2.2 | 2.3 | 2.4 | 4.4 |
| | | CPT (1850) | | | | 0.0955 | 0.236 | 0.4629 | 0.3732 | 0.5951 | 0.8926 | 1.3716 |
| | | Mindlin (1951) | | | | 0.0930 | 0.2219 | 0.4149 | 0.3406 | 0.5206 | 0.7446 | 1.0764 |
| | | Reddy (1984) | | | | 0.0931 | 0.2219 | 0.4150 | 0.3406 | 0.5208 | 0.7453 | 1.0785 |
| | | Ghugal & Sayyad (2011) | 0 | 0 | 0 | 0.0933 | 0.2231 | 0.4184 | 0.3431 | 0.5258 | 0.7542 | 1.0945 |
| | | Sayyad & Ghugal (2012) | | | | 0.0931 | 0.2223 | 0.4163 | 0.3415 | 0.5228 | 0.7499 | 1.0872 |
| | $w_w$ | Exact (1970) | | | | 0.0932 | 0.2226 | 0.4171 | 0.3421 | 0.5239 | 0.7511 | 1.0889 |
| | | Djidar et al. (2022) | | | | 0.0930 | 0.2220 | 0.4153 | 0.3408 | 0.5213 | 0.7464 | 1.0807 |
| | | Present | 0 | 0 | 0 | **0.0930** | **0.2220** | **0.4153** | **0.3408** | **0.5213** | **0.7464** | **1.0807** |
| | | | 10 | 2 | 0.01 | **0.0997** | **0.2279** | **0.4211** | **0.3466** | **0.5271** | **0.7525** | **1.0873** |
| | | | | | 0.05 | **0.1020** | **0.2289** | **0.4217** | **0.3472** | **0.5276** | **0.7528** | **1.0875** |
| | | | | | 0.1 | **0.1048** | **0.2301** | **0.4223** | **0.3480** | **0.5281** | **0.7531** | **1.0877** |
| | | CPT (1850) | | | | -- | -- | -- | -- | -- | -- | -- |
| | | Mindlin (1951) | | | | 3.2538 | 3.4112 | 3.6510 | 3.558 | 3.7842 | 4.072 | 4.5098 |
| | | Reddy (1984) | | | | 3.2555 | 3.4125 | 3.6517 | 3.5589 | 3.7848 | 4.072 | 4.5092 |
| | | Ghugal & Sayyad (2011) | 0 | 0 | 0 | 3.2469 | 3.394 | 3.6178 | 3.5312 | 3.7414 | 4.0082 | 4.4102 |
| | | Sayyad & Ghugal (2012) | | | | 3.2428 | 3.3994 | 3.6381 | 3.5455 | 3.7709 | 4.0576 | 4.4944 |
| | $w_\theta$ | Exact (1970) | | | | 3.2465 | 3.3933 | 3.6160 | 3.5298 | 3.7393 | 4.0037 | 4.4013 |
| | | Djidar et al. (2022) | | | | 3.2555 | 3.4123 | 3.6513 | 3.5586 | 3.7842 | 4.0712 | 4.5082 |
| | | Present | 0 | 0 | 0 | **3.2555** | **3.4123** | **3.6513** | **3.5586** | **3.7842** | **4.0712** | **4.5082** |
| | | | 10 | 2 | 0.01 | **3.2555** | **3.4123** | **3.6513** | **3.5586** | **3.7842** | **4.0712** | **4.5082** |
| | | | | | 0.05 | **3.2555** | **3.4123** | **3.6513** | **3.5586** | **3.7842** | **4.0712** | **4.5082** |
| 1 | | | | | 0.1 | **3.2555** | **3.4123** | **3.6513** | **3.5586** | **3.7842** | **4.0712** | **4.5082** |

Table 3 presents a comparison between the natural bending mode (NBM) frequencies and thickness shear mode (TSM) frequencies for simply supported isotropic square plates resting on a viscoelastic foundation. It is observed that the inclusion of viscosity leads to larger frequency values, indicating that the viscoelastic effect contributes to the stiffening of the plate.

*Table 4 – Comparison between the natural bending mode frequencies* $(\bar{\omega}_w)$ *and others found in others works, of simply supported isotropic rectangular plates*$(S = 10)$

| a/b | w | Theory | Kw | Ks | $\bar{C}_t$ | (m.n) | | | | | | |
|---|---|---|---|---|---|---|---|---|---|---|---|---|
| | | | | | | 1.1 | 1.2 | 1.3 | 2.2 | 2.3 | 2.4 | 3.2 |
| √2 | ww | CPT (1850) | 0 | 0 | 0 | 0.0718 | 0.1427 | 0.2591 | 0.2821 | 0.3958 | 0.5513 | 0.5073 |
| | | Mindlin (1951) | | | | 0.0703 | 0.1373 | 0.2424 | 0.2625 | 0.3595 | 0.4861 | 0.4509 |
| | | Reddy (1984) | | | | 0.0704 | 0.1374 | 0.2426 | 0.2628 | 0.3601 | 0.4874 | 0.4520 |
| | | Ghugal & Sayyad (2011) | | | | 0.0705 | 0.1393 | 0.2438 | 0.2642 | 0.3623 | 0.4906 | 0.4550 |
| | | Sayyad & Ghugal (2012) | | | | 0.0704 | 0.1376 | 0.2433 | 0.2639 | 0.3639 | 0.4928 | 0.4552 |
| | | Exact (1970) | | | | 0.0704 | 0.1376 | 0.2431 | 0.2634 | 0.3612 | 0.4890 | 0.4535 |
| | | Djidar et al. (2022) | | | | 0.0703 | 0.1373 | 0.2425 | 0.2627 | 0.3598 | 0.4867 | 0.4514 |
| | | Present | 0 | 0 | 0 | **0.0703** | **0.1373** | **0.2425** | **0.2627** | **0.3598** | **0.4867** | **0.4514** |
| | | | 10 | 2 | 0.01 | **0.0767** | **0.1419** | **0.2462** | **0.2676** | **0.3641** | **0.4907** | **0.4567** |
| | | | | | 0.05 | **0.0797** | **0.1435** | **0.2471** | **0.2684** | **0.3648** | **0.4912** | **0.4572** |
| | | | | | 0.1 | **0.0833** | **0.1455** | **0.2483** | **0.2695** | **0.3655** | **0.4917** | **0.4578** |

*Table 5 - Non-dimensional fundamental frequencies* $\tilde{\omega}$ *for isotropic square plates resting on the Visco-Winkler-Pasternak foundations (a/h = 5, i = j = 1).*

| $K_w$ | $K_s$ | Matsunaga (2000) | Thai and Choi (2012) | Mantari (2014) | Present | | | |
|---|---|---|---|---|---|---|---|---|
| | | | | | $\bar{C}_t$=0 | $\bar{C}_t$=0.5 | $\bar{C}_t$=1 | $\bar{C}_t$=1.5 |
| **0** | **0** | **17.526** | **17.4523** | **17.5271** | **17.45234** | **-** | **-** | **-** |
| **10** | | **17.7847** | **17.7248** | **17.7858** | **17.72445** | **17.72945** | **17.73445** | **17.73945** |
| **10^2** | | **19.9528** | **20.0076** | **19.9613** | **20.00731** | **20.01174** | **20.01616** | **20.02059** |
| **10^3** | | **34.3395** | **35.5039** | **34.7796** | **35.50397** | **35.50646** | **35.50895** | **35.51144** |
| **0** | **10** | **22.0429** | **22.2145** | **22.0707** | **22.21443** | **22.21842** | **22.22240** | **22.22639** |
| **10** | | **22.2453** | **22.4286** | **22.2757** | **22.42873** | **22.43268** | **22.43663** | **22.44057** |
| **10^2** | | **23.983** | **24.2723** | **24.0401** | **24.27221** | **24.27586** | **24.27950** | **24.28315** |
| **10^3** | | **36.6276** | **38.065** | **37.2169** | **38.06470** | **38.06702** | **38.06934** | **38.07166** |

Table 4 shows a comparison between the natural bending mode frequencies obtained with the model proposed in this study and those

reported in the literature for simply supported isotropic rectangular plates. The results obtained turn out to be in good agreement with those reported in other studies in which the viscosity term and elastic foundation parameters were neglected. Once again, increasing the damping coefficient leads to a stiffer plate response, with greater rigidity.

To further assess the accuracy of the proposed model, the first two non-dimensional natural frequencies of a thick square plate (a/h=5) resting on an elastic foundation are reported. In this context, the following parameters are considered:

$$\widetilde{\omega} = \omega a^2\sqrt{\rho_0 h/D_0}\ , D_0 = \frac{Eh^3}{12(1-v^2)}\ , K_w = \frac{k_w a^4}{D_0}\ , K_s = \frac{k_s a^2}{D_0}$$

$$f(z) = h\sinh\left(\frac{z}{h}\right) - \frac{4z^3}{3h^2}\cosh\left(\frac{1}{2}\right)$$

Tables 5 and 6 illustrate the validation of the proposed theory through a comparison with other higher-order shear deformation theories reported in the literature, specifically those by Thai and Choi (2012), Matsunaga (2000), and Mantari et al. (2014). The fundamental frequencies corresponding to the first mode (i=j=1), denoted by $\omega_{11}$, are presented in Table 5, whereas the natural frequencies $\omega_{12}$ are listed in Table 6.

*Table 6 - Non-dimensional fundamental frequencies $\widetilde{\omega}$ for isotropic square plates resting on the Visco-Winkler-Pasternak foundations (a/h = 5, i = j = 2).*

| $K_w$ | $K_s$ | Matsunaga (2000) | Thai and Choi (2012) | Mantari (2014) | Present | | | |
|---|---|---|---|---|---|---|---|---|
| | | | | | $\bar{C}_t$=0 | $\bar{C}_t$=1 | $\bar{C}_t$=2 | $\bar{C}_t$=3 |
| **0** | | **38.4827** | **38.1883** | **38.4991** | **38.18838** | **—** | **—** | **—** |
| **10** | | **38.5929** | **38.3098** | **38.6093** | **38.31023** | **38.31474** | **38.31924** | **38.32375** |
| **10^2** | **0** | **39.5669** | **39.3895** | **39.586** | **39.38973** | **39.39412** | **39.39850** | **39.40288** |
| **10^3** | | **47.8667** | **48.8772** | **48.1688** | **48.87732** | **48.88084** | **48.88436** | **48.88788** |
| **0** | | **43.4816** | **43.7943** | **43.5741** | **43.79477** | **43.79870** | **43.80264** | **43.80657** |
| **10** | | **43.5747** | **43.9009** | **43.6701** | **43.90089** | **43.90482** | **43.90874** | **43.91267** |
| **10^2** | **10** | **44.3994** | **44.8445** | **44.5241** | **44.84454** | **44.84839** | **44.85223** | **44.85607** |
| **10^3** | | **51.6029** | **53.358** | **52.2029** | **53.35832** | **53.36154** | **53.36476** | **53.36798** |

According to the results presented in Table 5, the fundamental frequencies obtained by the present model show very good agreement with the results of Thai and Choi (2014), particularly when the viscosity coefficient is zero. They are also slightly higher than those reported by Matsunaga (2000) and Mantari et al. (2014) for high values of the first coefficient of the parameter $K_w$. In addition, the fundamental frequencies

increase with the increase of the viscoelastic foundation parameters $K_w$, $K_s$ and $\bar{C}_t$. On the other hand, Table 6 also indicates that the results from the present shear deformation theory closely match those of the higher-order theories by Thai and Choi (2014), Matsunaga (2000), and Mantari et al. (2014). According to this comparison, taking into account the viscoelastic foundation parameters stiffens the plate, thereby increasing its fundamental frequencies.

## Conclusion

This study investigated the bending and free vibration behavior of simply supported isotropic plates resting on a viscoelastic Winkler–Pasternak foundation, using a refined two-variable higher-order shear deformation theory. The stress and displacement responses of the plates subjected to uniformly distributed loads (UDLs) and sinusoidally distributed loads (SDLs) were analyzed.

The proposed formulation was then validated against reported solutions. It showed excellent agreement with existing findings when the viscoelastic effects (*Kw*, *Ks*, *Ct* ) are neglected.

It was found that when the above-mentioned effects are included, the displacements and stresses are significantly reduced. In this case, the influence of the Pasternak shear modulus (*Ks*) is more significant than that of the Winkler modulus (*Kw*). Moreover, the inclusion of viscosity leads to increased natural frequencies, highlighting the stiffening effect of the viscoelastic foundation.

The present study, which demonstrates clear novelty and practical relevance, is an extension of previous works, such as that carried out by Djidar et al. (2022), as it performs a comprehensive parametric analysis and provides essential insights for the analysis of plates resting on viscoelastic foundations.

## *References*

Ait Atmane, H., Tounsi, A., Mechab, I., & Adda Bedia, E. A. (2010). Free vibration analysis of functionally graded plates resting on Winkler–Pasternak elastic foundations using a new shear deformation theory. *International Journal of Mechanics and Materials in Design*, 6, 113-121. Available at: https://doi.org/10.1007/s10999-010-9110-x

Ameur, M., Tounsi, A., Mechab, I., & El Bedia, A. A. (2011). A new trigonometric shear deformation theory for bending analysis of functionally graded plates resting on elastic foundations. *KSCE Journal of Civil Engineering*, *15*(8), 1405-1414.Available at: https://doi.org/10.1007/s12205-011-1361-z

Amini, M. H., Soleimani, M., &Rastgoo, A. (2009). Three-dimensional free vibration analysis of functionally graded material plates resting onan elastic foundation. *Smart Materials and Structures*, *18*(8), 085015.Available at: https://doi.org/10.1088/0964-1726/18/8/085015

Arani, A. G., &Kiani, F. (2018). Nonlinear free and forced vibration analysis of microbeams resting on the nonlinear orthotropic visco-Pasternak foundation with different boundary conditions. *Steel and Composite Structures*, *28*(2), 149-165. Available at: https://doi.org/10.12989/scs.2018.28.2.149.

Arshid, E., Khorshidvand, A. R., &Khorsandijou, S. M. (2019). The effect of porosity on free vibration of SPFG circular plates resting on visco-Pasternak elastic foundation based on CPT, FSDT and TSDT. *Structural Engineering and Mechanics, An Int'l Journal*, *70*(1), 97-112. Available at: https://doi.org/10.12989/sem.2019.70.1.097.

Baferani, A. H., Saidi, A. R., &Ehteshami, H. (2011). Accurate solution for free vibration analysis of functionally graded thick rectangular plates resting on elastic foundation. *Composite Structures*, *93*(7), 1842-1853. Available at: https://doi.org/10.1016/j.compstruct.2011.01.020

Benahmed, A., Houari, M. S. A., Benyoucef, S., Belakhdar, K., &Tounsi, A. (2017). A novel quasi-3D hyperbolic shear deformation theory for functionally graded thick rectangular plates on elastic foundation. *Geomech. Eng*, *12*(1), 9-34. Available at: https://doi.org/10.12989/gae.2017.12.1.009

Bennedjadi, M., Aldosari, S. M., Chikh, A., Kaci, A., Bousahla, A. A., Bourada, F., ... &Tounsi, A. (2023). Visco-elastic foundation effect on buckling response of exponentially graded sandwich plates under various boundary conditions. *Geomechanics and Engineering*, *32*(2), 159-177. Available at: https://doi.org/10.12989/gae.2023.32.2.159

Bouazza, M., Tounsi, A., Adda-Bedia, E. A., &Megueni, A. (2010). Thermoelastic stability analysis of functionally graded plates: An analytical approach. *Computational Materials Science*, *49*(4), 865-870. Available at: https://doi.org/10.1016/j.commatsci.2010.06.038

Boulefrakh, L., Hebali, H., Chikh, A., Bousahla, A. A., Tounsi, A., & Mahmoud, S. R. (2019). The effect of parameters of visco-Pasternak foundation on the bending and vibration properties of a thick FG plate. *Geomechanics and Engineering*, *18*(2), 161-178. Available at: https://doi.org/10.12989/gae.2019.18.2.161

Bounouara, F., Aldosari, S. M., Chikh, A., Kaci, A., Bousahla, A. A., Bourada, F., ... &Albalawi, H. (2023). The effect of visco-Pasternak foundation on the free vibration behavior of exponentially graded sandwich plates with various boundary conditions. *Steel and Composite Structures, An International Journal*, *46*(3), 367-383.Available at: https://doi.org/10.12989/scs.2023.46.3.367

Bounouara, F., Sadoun, M., Saleh, M. M. S., Chikh, A., Bousahla, A. A., Kaci, A., ... &Tounsi, A. (2023). Effect of visco-Pasternak foundation on thermo-mechanical bending response of anisotropic thick laminated composite plates. *Steel and Composite Structures*, *47*(6), 693-707. Available at: https://doi.org/10.12989/scs.2023.47.6.693

Chen, C. S. (2005). Nonlinear vibration of a shear deformable functionally graded plate. *Composite Structures*, *68*(3), 295-302. Available at: https://doi.org/10.1016/j.compstruct.2004.03.022

Chen, C. S., Hsu, C. Y., &Tzou, G. J. (2009). Vibration and stability of functionally graded plates based on a higher-order deformation theory. *Journal of reinforced plastics and composites*, *28*(10), 1215-1234. Available at: https://doi.org/10.1177/0731684408088884

Djidar, F. Z., Hebali, H., Amara, K., Touns, A., Bendaho, B., Ghazwani, M. H., & Hussain, M. (2022). Flexural and free vibration responses of thick isotropic bridge deck using a novel two variable refined plate theory. Available at: https://doi.org/10.12989/sem.2022.82.6.725

Fallah, A., Aghdam, M. M., &Kargarnovin, M. H. (2013). Free vibration analysis of moderately thick functionally graded plates on elastic foundation using the extended Kantorovich method. *Archive of Applied Mechanics*, *83*(2), 177-191. Available at: https://doi.org/10.1007/s00419-012-0645-1

Frahlia, H., Bennai, R., Nebab, M., AitAtmane, H., &Tounsi, A. (2023). Assessing effects of parameters of viscoelastic foundation on the dynamic response of functionally graded plates using a novel HSDT theory. *Mechanics of Advanced Materials and Structures*, *30*(13), 2765-2779. Available at: https://doi.org/10.1080/15376494.2022.2062632

Ghugal, Y. M., & Sayyad, A. S. (2011). Free vibration of thick orthotropic plates using trigonometric shear deformation theory. *Latin American Journal of Solids and Structures*, *8*, 229-243. Available at: https://doi.org/10.1590/S1679-78252011000300002

Ghugal, Y. M., &Pawar, M. D. (2011). Buckling and vibration of plates by hyperbolic shear deformation theory. *Journal of Aerospace Engineering and Technology*, *1*(1), 1-12. [online]. Available at: https://www.researchgate.net/profile/Yuwaraj-Ghugal/publication/285467416_Buckling_and_vibration_of_plates_by_hyperbolic_shear_deformation_theory/links/568113cb08ae051f9aec2333/Buckling-and-vibration-of-plates-by-hyperbolic-shear-deformation-theory.pdf [Accessed: 03 January 2025].

Grover, N., Maiti, D. K., & Singh, B. N. (2013). A new inverse hyperbolic shear deformation theory for static and buckling analysis of laminated composite and sandwich plates. *Composite Structures*, *95*, 667-675. Available at: https://doi.org/10.1016/j.compstruct.2012.08.012

Hebali, H., Tounsi, A., Houari, M. S. A., Bessaim, A., &Bedia, E. A. A. (2014). New quasi-3D hyperbolic shear deformation theory for the static and free vibration analysis of functionally graded plates. *Journal of Engineering Mechanics*, *140*(2), 374-383. Available at: https://doi.org/10.1061/(ASCE)EM.1943-7889.0000665

Huang, Z. Y., Lü, C. F., & Chen, W. Q. (2008). Benchmark solutions for functionally graded thick plates resting on Winkler–Pasternak elastic foundations. *Composite Structures*, *85*(2), 95-104. Available at: https://doi.org/10.1016/j.compstruct.2007.10.010

Karama, M., Afaq, K.S., Mistou, S. (2003), Mechanical behaviour of laminated composite beam by the new multilayered laminated composite structures model with transverse shear stress continuity. *Int. J. Solids Struct.*, 40(6), 1525–1546. Available at: https://doi.org/10.1016/S0020-7683(02)00647-9

Kiani, Y., &Eslami, M. R. (2012). Thermal buckling and post-buckling response of imperfect temperature-dependent sandwich FGM plates resting on elastic foundation. *Archive of Applied Mechanics*, *82*(7), 891-905. Available at: https://doi.org/10.1007/s00419-011-0599-8

Kirchhoff, G. (1850). Über das Gleichgewicht und die BewegungeinerelastischenScheibe. *Journal für die reine und angewandte Mathematik (Crelles Journal)*, *1850*(40), 51-88. Available at: https://doi.org/10.1515/crll.1850.40.51

Kirchhoff, G. (1850). Ueber die Schwingungen einer kreisförmigen elastischen Scheibe. *Annalen der PhysikundChemie*, *81*, 258-264. Available at: https://doi.org/10.1002/andp.18501571005

Lanhe, W. (2004). Thermal buckling of a simply supported moderately thick rectangular FGM plate. *Composite Structures*, *64*(2), 211-218. Available at: https://doi.org/10.1016/j.compstruct.2003.08.004

Lee, K. H., Senthilnathan, N. R., Lim, S. P., and Chow, S. T. (1989). A simple Higher Order Nonlinear Shear Deformation Plate Theory. *International Journal of Nonlinear Mechanics,* 24 (2), 127–137. Available at: https://doi.org/10.1016/0020-7462(89)90004-8

Levy, M. (1877). Mémoire sur la théorie des plaques élastiques planes. *Journal de mathématiques pures et appliquées*, 30, 219-306. [online]. Available at: https://www.numdam.org/item/JMPA_1877_3_3__219_0.pdf [Accessed: 01 May 2025].

Mahi, A., El Abbas,A.B., Tounsi, A. (2015). A new hyperbolic shear deformation theory for bending and free vibration analysis of isotropic, functionally graded, sandwich and laminated composite plates. *Applied Mathematical Modelling*, 39(9), 2489–2508. Available at: https://doi.org/10.1016/j.apm.2014.10.045

Mantari, J. L., Oktem, A. S., &Soares, C. G. (2012). A new trigonometric shear deformation theory for isotropic, laminated composite and sandwich plates. *International Journal of Solids and Structures*, *49*(1), 43-53. Available at: https://doi.org/10.1016/j.ijsolstr.2011.09.008

Mantari, J. L., &Soares, C. G. (2012). Bending analysis of thick exponentially graded plates using a new trigonometric higher order shear deformation theory. *Composite Structures*, *94*(6), 1991-2000. Available at: https://doi.org/10.1016/j.compstruct.2012.01.005

Mantari, J. L., Granados, E. V., &Soares, C. G. (2014). Vibrational analysis of advanced composite plates resting on elastic foundation. *Composites Part B: Engineering*, *66*, 407-419. Available at: https://doi.org/10.1016/j.compositesb.2014.05.026

Mantari, J. L., Granados, E. V., Hinostroza, M. A., & Soares, C. G. (2014). Modelling advanced composite plates resting on elastic foundation by using a

quasi-3D hybrid type HSDT. *Composite Structures*, 118, 455-471. Available at: http://dx.doi.org/10.1016/j.compstruct.2014.07.039

Matsunaga, H. (2000). Vibration and stability of thick plates on elastic foundations. *Journal of engineering mechanics,* 126(1), 27-34. Available at: https://doi.org/10.1061/(ASCE)0733-9399(2000)126:1(27)

Mindlin, R. (1951). Influence of rotatory inertia and shear on flexural motions of isotropic, elastic plates.*J. of Appl. Mechanics,* 18, 31-38 .Available at: https://doi.org/10.1115/1.4010217

Mudhaffar, I. M., Chikh, A., Tounsi, A., Al-Osta, M. A., Al-Zahrani, M. M., & Al-Dulaijan, S. U. (2023). Impact of viscoelastic foundation on bending behavior of FG plate subjected to hygro-thermo-mechanical loads. *Structural Engineering and Mechanics, An Int'l Journal*, *86*(2), 167-180. Available at: https://doi.org/10.12989/sem.2023.86.2.167

Pagano, N. J. (1970). Exact solutions for bidirectional composites and sandwich plates. *Journal of Composite Materials*, 4(1), 20–34. Available at: https://doi.org/10.1177/002199837000400102

Park, J. S., & Kim, J. H. (2006). Thermal postbuckling and vibration analyses of functionally graded plates. *Journal of Sound and Vibration*, *289*(1-2), 77-93. Available at: https://doi.org/10.1016/j.jsv.2005.01.031

Reddy, J. N. (1984). A simple higher-order theory for laminated composite plates.*ASME Journal of Applied Mechanics*, 51, 745–752. Available at: https://doi.org/10.1115/1.3167719

Saidi, H., Tounsi, A., &Bousahla, A. A. (2016). A simple hyperbolic shear deformation theory for vibration analysis of thick functionally graded rectangular plates resting on elastic foundations. *Geomechanics & engineering*, *11*(2), 289-307. Available at: https://doi.org/10.12989/gae.2016.11.2.289

Sayyad, A. S., &Ghugal, Y. M. (2012). Bending and free vibration analysis of thick isotropic plates by using exponential shear deformation theory. *Applied and Computational mechanics*, *6*(1). [online]. Available at: https://acm.kme.zcu.cz//article/view/171 [Accessed: 05 January 2025].

Shimpi, R. P. (2002). Refined plate theory and its variants. *AIAA journal*, *40*(1), 137-146.Available at: https://doi.org/10.2514/2.1622

Sobhy, M. (2013). Buckling and free vibration of exponentially graded sandwich plates resting on elastic foundations under various boundary conditions. *Composite Structures*, *99*, 76-87. Available at: https://doi.org/10.1016/j.compstruct.2012.11.018

Soldatos, K. (1992). A transverse shear deformation theory for homogeneous monoclinic plates. *Acta Mechanica*, *94*(3), 195-220. Available at: https://doi.org/10.1007/BF01176650

Stein, M. (1986). Nonlinear theory for plates and shells including the effects of transverse shearing. *AIAA journal*, *24*(9), 1537-1544. Available at: https://doi.org/10.2514/3.9477

Stein, M. (1989). Vibration of beams and plate strips with three-dimensional flexibility. *ASME Journal of Applied Mechanics,* Brief Notes,56(1), 228–231. Available at: https://doi.org/10.1115/1.3176054

Stein, M., Sydow, P. D., &Librescu, L. (1990). Postbuckling of long thick plates in compression including higher order transverse shearing effects. In *Studies in Applied Mechanics*, (24), 63-86. Elsevier. Available at: https://doi.org/10.1016/B978-0-444-88366-7.50008-7

Thai, H. T., & Choi, D. H. (2012). A refined shear deformation theory for free vibration of functionally graded plates on elastic foundation. *Composites Part B: Engineering*, 43(5), 2335-2347. Available at: https://doi.org/10.1016/j.compositesb.2011.11.062

Wattanasakulpong, N., Prusty, G. B., & Kelly, D. W. (2013). Free and forced vibration analysis using improved third-order shear deformation theory for functionally graded plates under high temperature loading. *Journal of Sandwich Structures & Materials*, *15*(5), 583-606. Available at: https://doi.org/10.1177/1099636213495751

Winkler, E. (1867). *Die Lehre von der Elasticitaet und Festigkeit*, Prag Dominicus. [e-book]. Available at: https://books.google.com/books?id=i2kSAAAAIAAJ [Accessed: 15 March 2025].

Xiang, S., Jin, Y. X., Bi, Z. Y., Jiang, S. X., & Yang, M. S. (2011). A n-order shear deformation theory for free vibration of functionally graded and composite sandwich plates. *Composite Structures*, *93*(11), 2826-2832.Available at: https://doi.org/10.1016/j.compstruct.2011.05.022

Xiang, S., & Kang, G. W. (2013). Static analysis of functionally graded plates by the various shear deformation theory. *Composite Structures*, *99*, 224-230. Available at: https://doi.org/10.1016/j.compstruct.2012.11.021

Yaghoobi, H., &Yaghoobi, P. (2013). Buckling analysis of sandwich plates with FGM face sheets resting on elastic foundation with various boundary conditions: an analytical approach. *Meccanica*, *48*(8), 2019-2035. Available at: https://doi.org/10.1007/s11012-013-9720-0

Younsi, A., Tounsi, A., Zaoui, F. Z., Bousahla, A. A., & Mahmoud, S. R. (2018). Novel quasi-3D and 2D shear deformation theories for bending and free vibration analysis of FGM plates. *Geomechanics & engineering*, *14*(6), 519-532. Available at: https://doi.org/10.12989/gae.2018.14.6.519.

Zeighampour, H., &Beni, Y. T. (2015). Free vibration analysis of axially functionally graded nanobeam with radius varies along the length based on strain gradient theory. *Applied Mathematical Modelling*, *39*(18), 5354-5369. Available at: https://doi.org/10.1016/j.apm.2015.01.015

Zenkour, A. M. (2016). Buckling of a single-layered graphene sheet embedded in visco-Pasternak. *Advances in nano research*, *4*(4), 309. Available at: https://doi.org/10.12989/anr.2016.4.4.309.

# Uticaj parametara viskoelastične Pasternakove osnove na savijanje i vibraciono ponašanje debelih izotropnih ploča

*Hebali* Habib[a], *Djidar* Fatima Zohra[b], **autor za prepisku**, *Derras* Abdelhak[c]

[a] Mustapha Stambouli University, Departement of Civil Engineering, Mascara, People's Democratic Republic of Algeria

[b] Mustapha Stambouli University, Department of Civil Engineering, Mascara, People's Democratic Republic of Algeria +
Smart Structures Laboratory (SSL), University of Ain Temouchent, Ain Temouchent, People's Democratic Republic of Algeria

[c] Ahmed Ben Bella University – Oran 1, Department of Chemistry, Oran, People's Democratic Republic of Algeria +
Smart Structures Laboratory (SSL), University of Ain Temouchent, Ain Temouchent, People's Democratic Republic of Algeria

OBLAST: građevinarstvo
KATEGORIJA (TIP) ČLANKA: originalni naučni rad

*Sažetak:*

*Uvod/cilj: Primarni cilj ove studije je ispitivanje uticaja parametara viskoelastične Pasternakove podloge na ponašanje debelih izotropnih ploča sa prostim oslanjanjem pri savijanju i slobodnim vibracijama primenom teorije smične deformacije višeg reda sa dve nepoznate veličine (eng. HSDT). Usvojena teorija koristi ograničen broj nepoznatih i izbegava upotrebu korekcionih faktora smicanja kako bi poprečni smični naponi na površinama ploče bili jednaki nuli, što nije slučaj kod drugih teorija višeg reda koje uglavnom obuhvataju četiri ili pet nepoznatih. Pored toga, analiziraju se naponski i pomerajni odzivi pri dejstvu ravnomerno raspodeljenih opterećenja (eng. UDL) i sinusoidalno raspodeljenih opterećenja (eng. SDL). Takođe, prikazane su sopstvene frekvencije koje odgovaraju kako modovima savijanja tako i modovima smicanja po debljini kako bi se pokazala tačnost predloženog modela u predviđanju dinamičkog ponašanja kvadratnih i pravougaonih izotropnih ploča sa prostim oslanjanjem.*

*Metode: Glavni doprinos ovog rada ogleda se u uključivanju uticaja parametara elastične podloge i koeficijenata prigušenja na odzive debelih izotropnih ploča sa prostim oslanjanjem pri savijanju i vibracijama primenom usavršene teorije smične deformacije višeg reda sa dve nepoznate veličine. Pored toga, formulacija polja pomeranja uvodi određeni broj neodređenih integralnih članova, čime se smanjuje broj nepoznatih. Osnovne jednačine izvode se primenom Hamiltonovog principa. Zatim se koristi Navijeov metod za određivanje analitičkih rešenja za ploče sa prostim oslanjanjem, dok se sopstvene frekvencije izračunavaju rešavanjem odgovarajućeg problema sopstvenih vrednosti.*

*Rezultati: Analitički rezultati validirani su poređenjem sa nekoliko poznatih teorija smične deformacije višeg reda (eng. ESDT, HSDT, TSDT), teorijom*

*smične deformacije prvog reda (eng. FSDT) i klasičnom teorijom ploča (eng. CPT). Rezultati pokazuju odlično slaganje kada se viskoelastični efekti i efekti podloge ne uzimaju u obzir. Važno je naglasiti da rezultati pokazuju povećanu krutost ploče kada se ovi efekti uzmu u obzi, što dovodi do manjih ugiba i viših sopstvenih frekvencija.*

*Zaključak: Predložena teorija daje rezultate koji se dobro podudaraju sa rezultatima dobijenim primenom postojećih modela. Takođe, teorija jasno ukazuje na značajan uticaj parametara viskoelastične podloge na statičko i dinamičko ponašanje izotropnih ploča.*

*Ključne reči: savijanje, vibracije, izotropna ploča, visko-Pasternakove podloge.*

Paper received on: 20 June 2025.
Manuscript corrections submitted on: 21 November 2025.
Paper accepted for publishing on: 23 January 2026.

© 2026 The Authors. Published by Vojnotehnički glasnik / Military Technical Courier (www.vtg.mod.gov.rs). This article is an open access article distributed under the terms and conditions of the Creative Commons Attribution license (http://creativecommons.org/licenses/by/4.0/rs/).